

A study of the 100 Class Multi Beam Forming Technology and the Beam Forming Experiments

Teruaki ORIKASA and Yoshiyuki FUJINO

Satellite antenna for STICS is consists of the deployable reflector and the phased array feed and performs the multi beam formation with the number of array elements and beams are about 100 respectively. Partial model was developed for functional confirmation of digital beam former and digital channelizer (DBF/channelizer). DBF/channelizer has excellent flexibility for beam shaping function. We combined the partial model of array feed, reflector and DBF/channelizer and measured the radiation pattern of that antenna and discuss the function of DBF/channelizer for 100 class multi beam forming function.

1 Introduction

The STICS is considering developing a communication system using a multibeam antenna capable of forming about 100 beams. To effectively use beam frequencies, we primarily take an approach of frequency reuse. An antenna to be mounted on a satellite is expected to be a reflector antenna with a deployable, 30-m-class aperture mesh so that it fits in a rocket to be launched and deploys when the satellite reaches orbit. As the antenna feed system is comprised of a 100-element-class, phased-array antenna, and is controlled by a Digital Beam Former (DBF), it has a high degree of freedom for excitation weight and is capable of easily forming many beams. The STICS has developed a partial model of the DBF/channelizer. We are also developing a 16-element array feed. Here, we describe the results and evaluation of the experiments in which we simultaneously formed 100 beams using the DBF/channelizer

we developed toward the realization of a multibeam technology.

2 Study of multibeam forming technology

The 100-beam-class antenna we are studying will have a very complex Beam Forming Network (BFN) if we use a conventional multibeam antenna (analog system). Considering that the antenna will be mounted on a satellite, there are major technological issues such as its great mass, the large amount of power it consumes, and its substantial heat exhaustion.

The STICS is studying a satellite antenna to be mounted on the Engineering Test Satellite VIII (ETS-VIII)^{[1][2]} system while applying a DBF as the feed array's BFN. It is expected

Table 1 Antenna parameter

Parameter	value
Location of geostationary orbit [$^{\circ}$ E]	136.0
Frequency [MHz]	1995.1
Aperture diameter [m]	27.0
F/D	0.6
Focal length [m]	1.0
Boresight direction [east longitude degree], [north latitude degree]	135.0, 35.0
Number of beam	83
Diameter of beam (area) [degree]	0.45
Number of elements	127
Interval of element position [mm]	150.0

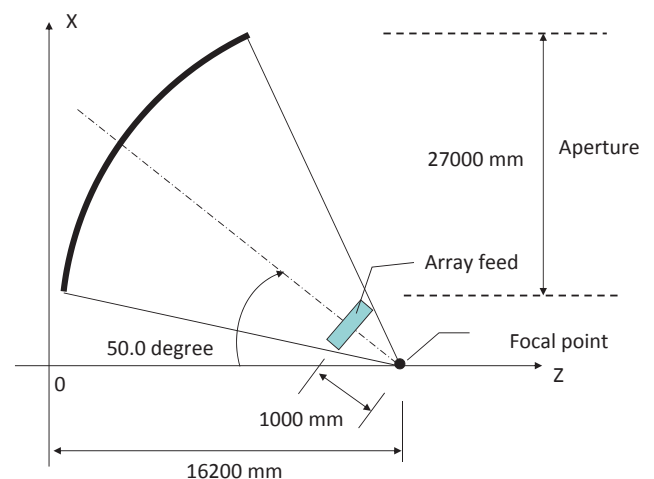


Fig. 1 Antenna parameter

to be feasible to reduce the mass of the DBF as it has a high degree of freedom, is easy to handle in terms of beam setting, and has a simplified feeding circuit.

In the experiments, we used a small-scale receiving DBF/channelizer developed by the STICS. This model has 16 input ports and 16 beam output ports. In addition, as it has 16 array feed elements, we checked the beam forming function of the DBF/channelizer primarily using a 16-element array feed.

We conducted the following two tests:

- (1) beam forming function test, and
- (2) 100 class multibeam forming test.

2.1 Study on the antenna-mounting-position of a satellite and beam formation

Taking into account the anticipated service areas on the earth and the antenna to be used, and based on the feed system baseline estimated in Subsection 3.2, we will set up specific parameters and check the characteristics of the DBF/channelizer. Parameter values set up are shown in Table 1 while antenna parameters calculated based on the values in Table 1 are shown in Fig. 1.

Based on these parameters, we considered locations from which beams are radiated across Japan’s mainland and surrounding waters. As satellite antennae are normally mounted either on the east or west side panel of a satellite, we carried out a study assuming these two mounting sides. Figures 2 and 3 show the results.

Red circles in the diagrams indicate the positions from which beams were set to be radiated. Based on this assumption, we determined excitation weight and calculated radiation patterns, which are indicated by white contour lines. Table 2 shows the azimuth and elevation angle under study of beam position viewed from geostationary orbit.

Through comparison of these figures, it was found that when an antenna is mounted on the east side of the satellite, characteristics and symmetry of radiation patterns were identified more precisely on the east side of the geographical range. In contrast, when an antenna is mounted on the west side of the satellite, radiation pattern characteristics were identified more precisely on the west side of the geographical range. Figures 4 and 5 show radiation patterns including sidelobes. In the case of Beam 3, the sidelobe level was higher in the pattern associated with the antenna mounted on the west side than the pattern associated with the antenna mounted on the east side. In contrast, concerning Beam 4, which is radiated from the west side of the geographical range, the sidelobe level was

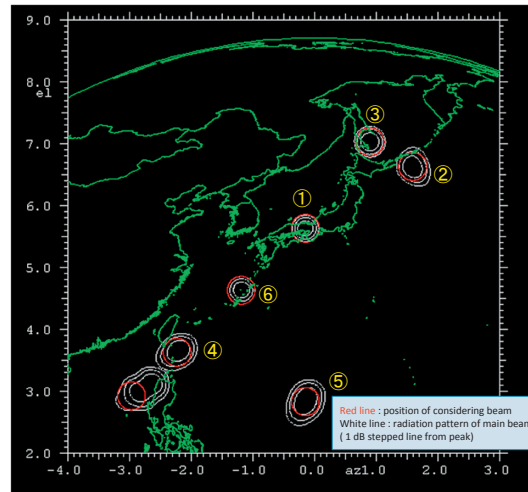


Fig. 2 Beam radiation pattern as perceived by the antenna mounted on the east side of the satellite

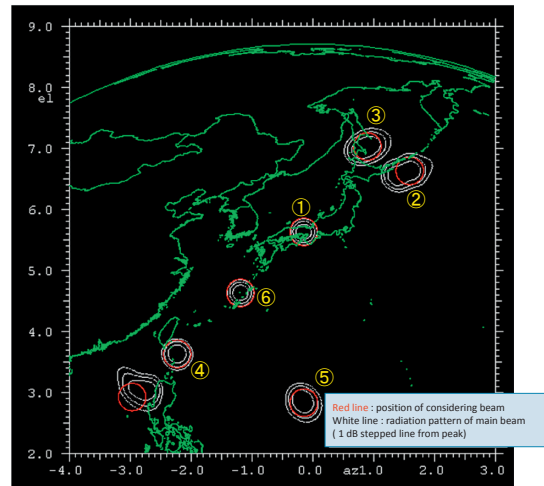


Fig. 3 Beam radiation pattern as perceived by the antenna mounted on the west side of the satellite

Table 2 Considering beam number and position

Beam number	Az [degree]	El [degree]
①	-0.14	5.63
②	1.59	6.62
③	0.89	7.03
④	-2.22	3.63
⑤	-0.14	2.83

higher in the pattern associated with the antenna mounted on the east side of the satellite than the pattern associated with the antenna mounted on the west side of the satellite. These results are attributed to the fact that individual beams use different parts of the reflector surface whose degree of curvature increases in the area closer to the feed system. For example, when an antenna is mounted on the west side of the satellite, beams that come from the east side of the geographical range tend to use the area of the

reflector surface with a large amount of curvature, while beams that come from the west side of the geographical range tend to use the distant, mirror-surfaced area of the reflector surface with a small amount of curvature. We think that the difference in radiation pattern characteristics is attributed to the different degrees of curvature on the different areas of mirror surface of the parabolic antenna.

From the studies above, it was found that the antenna responds differently to the beams that come from the east and west sides of the geographical range depending on the side of the satellite on which the antenna is mounted. In reality, when designing an antenna to be mounted on a satellite, it is necessary to consider the following:

- If it is important to enhance the characteristics of beams radiated from the west side of the geographical range, an antenna ought to be mounted on the west side of the satellite.
- If it is important to enhance the characteristics of beams radiated from the east side of the geographical range, an antenna ought to be mounted on the east side of the satellite.

2.2 Confirming beam forming function

To confirm that the DBF/channelizer we developed possesses beam forming capability equivalent to a 100-element-class array antenna, we measured its beam forming pattern while combining it with a 16-element array

feed, using a near-field antenna measurements (NFM) facility available at the NICT Kashima Space Technology Center. Taking into account the pattern measurement results of feeder and combining a reflector into the 127-element array feed antenna with 27-m aperture size, we evaluated the characteristics of the antenna.

Because there were 16 elements in the feed system, and the DBF/channelizer was compatible with 16 elements, we divided a 127-element array feed into smaller subarrays for evaluation and measurement purposes. Figure 6 depicts the array feed, which we expect to be used, and the scheme of dividing it into subarrays. Subarray groups, each consisting of up to 16 elements, were discerned by different colors. Individual groups were subject to repeated measurements to understand their patterns. Figure 7 compares the actual array feed to be measured with a subarray. When necessary, we selected an excitation element and set up excitation weight.

Figure 8 shows the procedure we followed. As the array to be measured possessed up to 16 elements, we divided it into subarrays as indicated in Fig. 6. We measured excita-

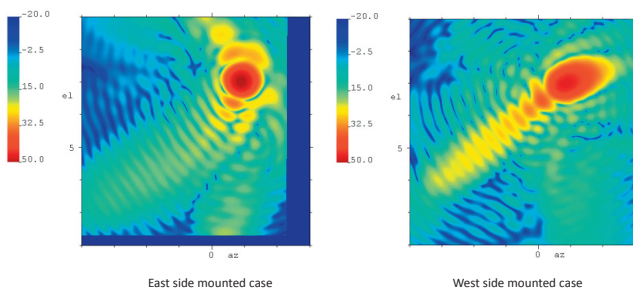


Fig. 4 Radiation pattern of beam ③

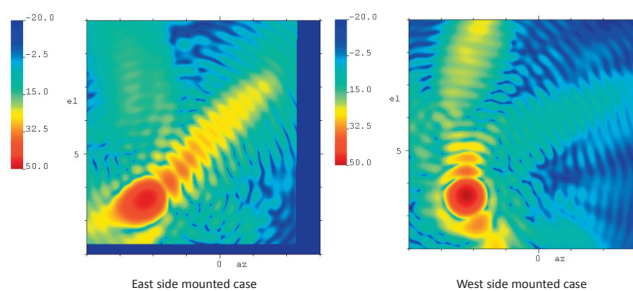


Fig. 5 Radiation pattern of beam ④

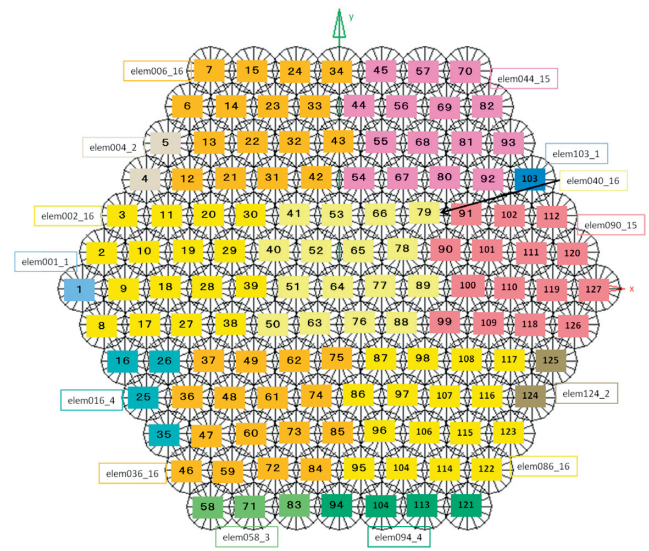
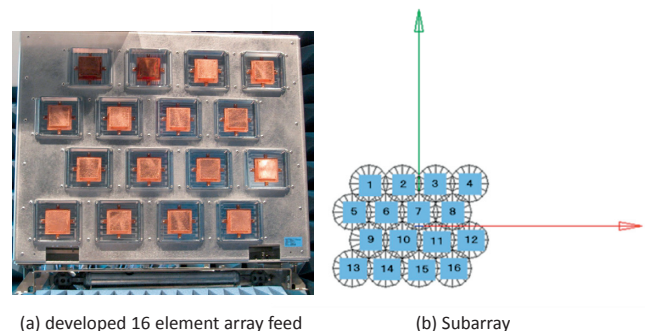


Fig. 6 Array feed and subarray



(a) developed 16 element array feed (b) Subarray
Fig. 7 Developed 16 element array feed and subarray

tion distribution patterns of elements in subarray groups assuming that excitation weights of the subarrays are the same as the excitation weight of the 127-element array. Then, we changed the excitation weight of the 16-element array feed in each subarray group, and measured individual groups based on these weight changes. We considered pattern measurement results of different subarrays as separate single-element patterns, and defined them as subarray element patterns. We determined the radiation pattern of the 127-element array feed by synthesizing these subarray element patterns without taking coupling between element groups into account. The center of each subarray is the same as the center of the subarray element patterns measured. This center is the position of the subarray elements. We calculated the pattern of this feed system and the pattern of this feed system combined with a 27-m-aperture reflector, and compared them with the pattern based solely on the original calculations. We use the reflector based on these parameters shown in Fig. 1 for pattern calculation, in which an ideal parabolic reflector was assumed.

The study results are described in Section 3.

2.3 Confirming multibeam forming function

The STICS is assuming to realize 100 multibeams. To determine whether the DBF/channelizer we developed possesses the basic function of simultaneously forming 100 beams, we combined a 16-element array feed with a mesh reflector, and carried out an experiment to determine whether the array feed combined with the DBF/channelizer forms 100 beams using the channelizer function of DBF/

channelizer. We took measurements using a plane polar near-field antenna measurement facility at Kyoto University’s Research Institute for Sustainable Humanosphere.

We checked the capability of the 16-element and 16-beam-compatible receiving DBF/channelizer we developed to form 100 beams by taking simultaneous measurements at seven different frequencies using the measurement facility. In this case, simultaneous measurements at seven frequencies were achieved by receiving signals while switching frequency at high speed using measurement system function so that the seven frequencies occurred in synchrony. Figure 9 shows a functional schematic of the array feed and DBF/channelizer when pattern measurements are taking place. As we used a receiving DBF/channelizer in this experiment, here, we explain the process in an order consistent with the receiving system.

The array feed receives signals at the frequencies of f_1, f_2, \dots and f_7 . Each element receives the signals and sends them to the digital channelizer. The channelizer separates each element signal into bands by a filter, and compiles element signals of the same frequency in chronological order. The DBF processes the frequency-specific signals using a DBF coefficient preset for each element, and outputs the signals in the forms of Beam 1 through Beam 7. To form 100 beams, 100 kinds of DBF coefficients need to be set. However, the memory of the DBF/channelizer we developed allows forming only 16 beams, and therefore does not permit simultaneous formation of 100 beams. This issue can be resolved by simply increasing the amount of memory and the number of ports. Thus, to confirm the capability of the DBF/channelizer to simultaneously form 100 beams, we increased the amount of memory and conducted evaluation based on repeated measurements. The DBF/channelizer possesses 16 ports and therefore is capable of outputting 16 beams. However, due to the

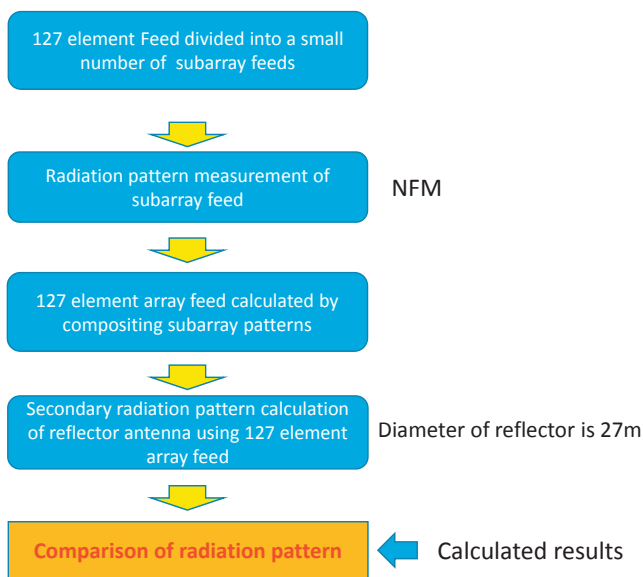


Fig. 8 Evaluation flow of beam forming function

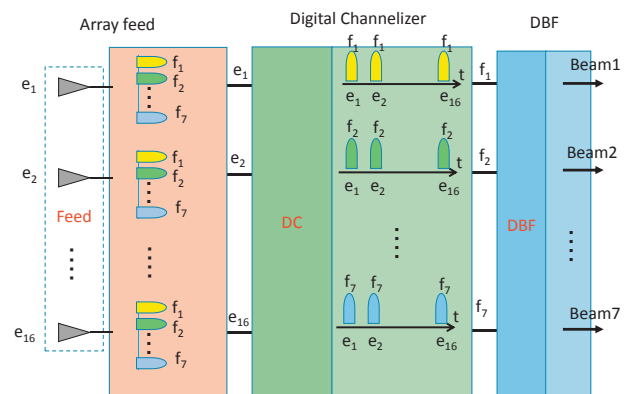


Fig. 9 Diagram of function of array feed and DBF/channelizer

constraint of the pattern measurement system, we measured each beam one by one by changing frequency. The DBF/channelizer is capable of outputting distinctive beams even if it processes input signals of the same frequency, by changing DBF coefficients. For example, when the DBF/channelizer processes signals with the uniform frequency of f_1 , it is capable of outputting distinctive beams in the forms of Beam 1-a, Beam 1-b, Beam 1-c, and so on.

In this experiment, we simultaneously measured up to seven different beams (i.e., seven different frequencies) and repeated the measurements while changing DBF coefficients a dozen or so times to obtain 100 beam patterns.

3 Results and discussion

In this section, we summarized the results and discussion concerning the two aspects of multibeam forming technology. We performed two separate experiments in which measurements were taken at different locations, namely: an experiment to confirm the beam forming function performed at the Kashima Space Technology Center (planar near-field antenna measurement facility), and an experiment to confirm the multibeam forming function performed at Kyoto University's Research Institute for Sustainable Humansphere (plane polar near-field antenna measurement facility). A special note is that the latter experiment was performed by combining a 3.3-m-aperture mesh reflector with a 16-element feed system and DBF/channelizer.

3.1 Experiment to confirm beam forming function

We confirmed the beam forming function of the DBF/channelizer we developed by measuring the radiation patterns using a planar NFM system available in Kashima. As described in Subsection 2.2, we took measurements on

subarrays containing up to 16 elements. Based on these measurements, we calculated the secondary radiation pattern of the 27-m-aperture reflector antenna, and made evaluation by comparing measured patterns with calculated patterns.

The schematic of the experiment using a planar NFM device is shown in Fig. 10. The blue frame represents equipment installed in an anechoic chamber including the feed system. The red and green frames represent the DBF/channelizer and measurement equipment, respectively. The six beams indicated in Figs. 2 and 3 were studied. Figure 11 shows a beam arrangement, beam positions we focused on, and beam cutting directions. The measurement of subarray

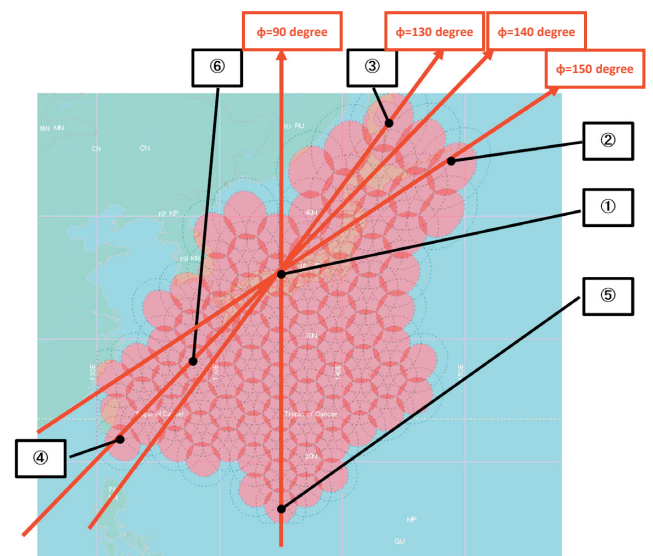


Fig. 11 Beam allocation and cut plane of radiation pattern

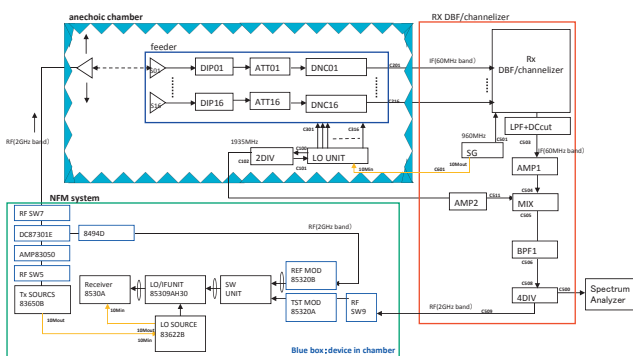


Fig. 10 Diagram of experiment of beam forming function

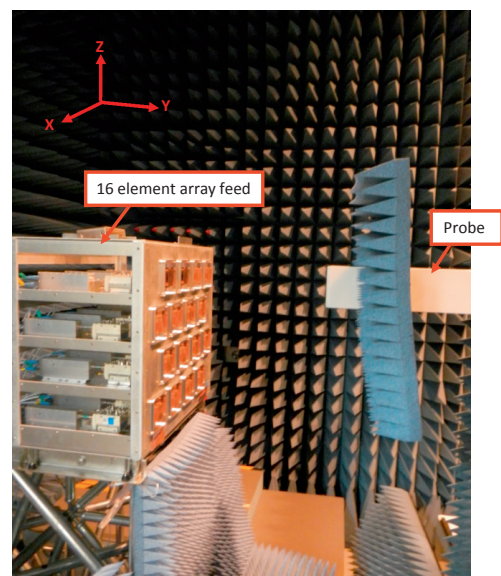
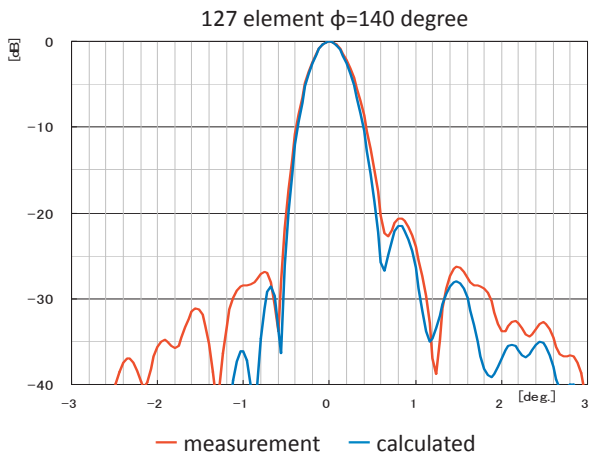
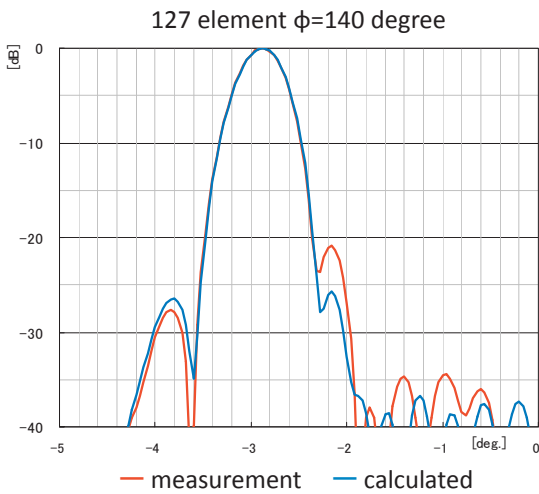


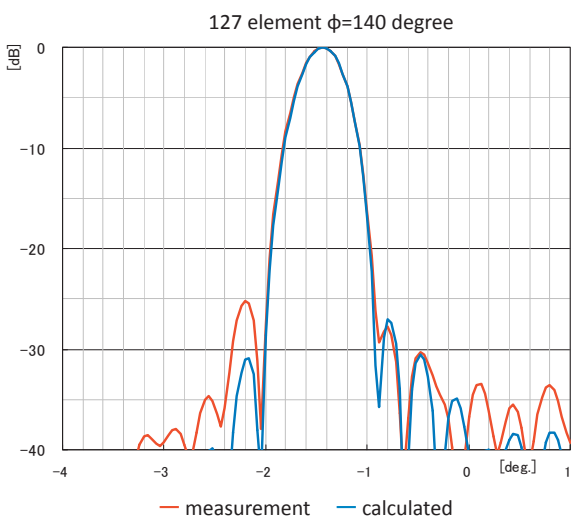
Fig. 12 General view of subarray measurement



(a) Cut pattern of Beam ①



(b) Cut pattern of Beam ④



(c) Cut pattern of Beam ⑥

Fig. 13 Evaluation results of secondary radiation pattern

patterns using the NFM system is depicted in Fig. 12.

Figure 13 illustrates the comparison between measurement results and calculation results. These results are based on cut planes of Beams 1, 4 and 6 with the angle of 140°. Blue and red lines represent calculated values and measurement results, respectively. In the main beam, calculated values and measured values coincided well. Similarly, the two types of values nearly matched in sidelobes that are equal to or less than -20 dB, indicating that they form beams. Based on this study, we confirmed that the DBF/channelizer is capable of setting excitation weight.

3.2 Experiment to confirm multibeam forming function

To confirm whether the DBF/channelizer is capable of forming approximately 100 beams, we combined a 16-element array feed with a mesh reflector, and carried out an experiment to examine its DBF/channelizer function using

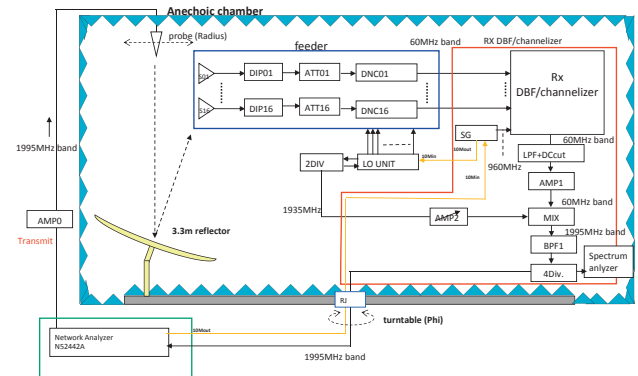


Fig. 14 Diagram of 100 class multi beam forming function experiment

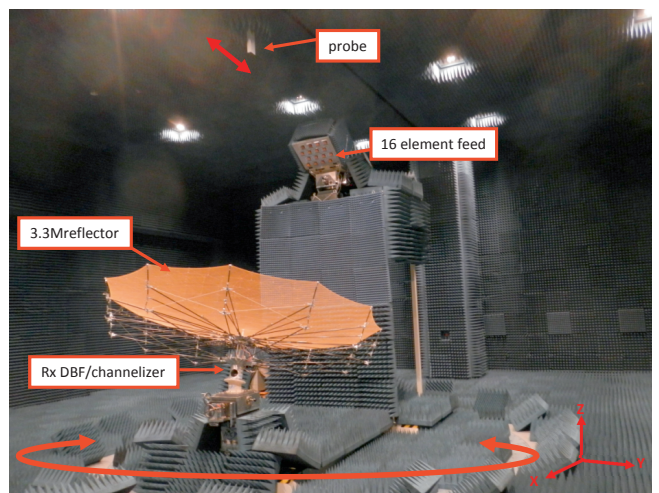


Fig. 15 Setup for the experiment to confirm multibeam forming function

Kyoto University’s antenna measurement facility. The arrangement of the measurement system is shown in Fig. 14. The plane polar near-field equipment, which includes a probe installed on a ceiling and is a single-axis drive system, is used to rotate and scan an antenna set on the floor. This equipment is capable of multifrequency simultaneous measurement in a single scan through high-speed switching of the frequency. Using this function, we made measurements at seven different frequencies at maximum in one try. The actual setting of the measurement system is shown in Fig. 15.

In the experiment, we actually measured about 100 beam patterns by changing DBF coefficients of the DBF/channelizer, thereby providing excitation weights of different arrays. Figure 16 illustrates beam arrangement. The circles indicate beam positions and numbers in the circles denote beam numbers. The colors of the circles representing Beam b001 through b100 in the red frame indicate different frequencies, and the measurement system simultaneously measured seven different frequencies and seven different beams. The beam interval was set to be 0.35°. The parameters of the antenna are shown in Fig. 17.

The position of the feed system is set 1.0 m away from the focal position toward the center of the reflector.

Measurement results are presented in Fig. 18. These results were nearly consistent with the expected beam position. Amplitude values represented by the vertical axis of the graph indicated that the beams were arranged at an interval of 0.35°. As this beam width is too wide for a 3.3-m-aperture antenna, the vertical axis was extended to

-1 dB for easier viewing. The view angle is shown in Fig. 18 based on the beam cutting direction of 30° indicated in Fig. 16. To compare cut patterns with calculated values using selected beams, we performed comparison and evaluation among Beams 11, 22, 59 and 79 including sidelobes. These results are shown in Fig. 19. Cut patterns of these beams were mostly consistent including sidelobes, indicating that the intended excitation weight was established. Based on the fact that similar results were also obtained for other beams, we concluded that the DBF/channelizer we developed is capable of forming approximately 100 beams.

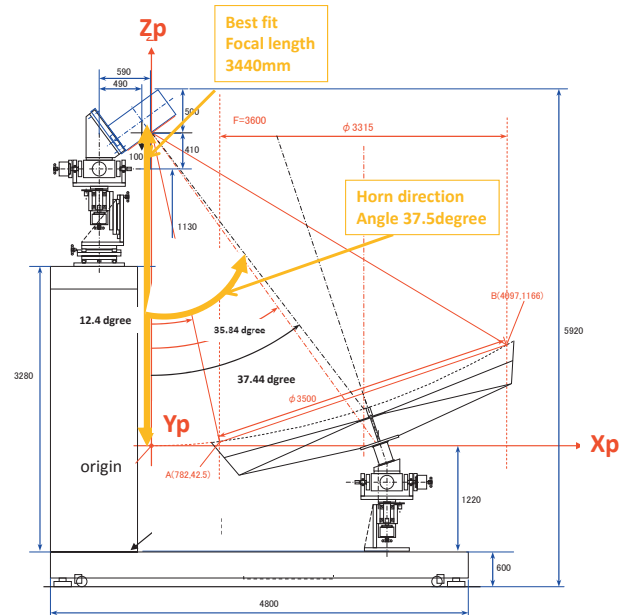


Fig. 17 Antenna parameter of measured antenna

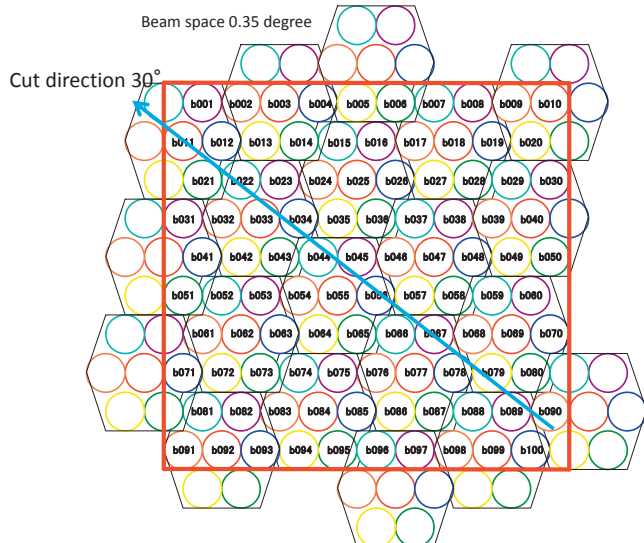


Fig. 16 Measurement beam allocation and cut plane

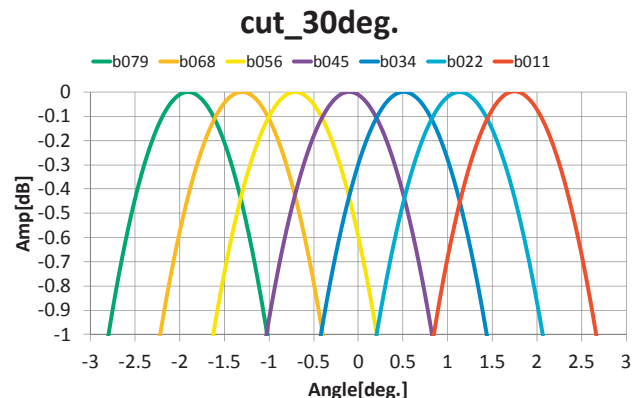
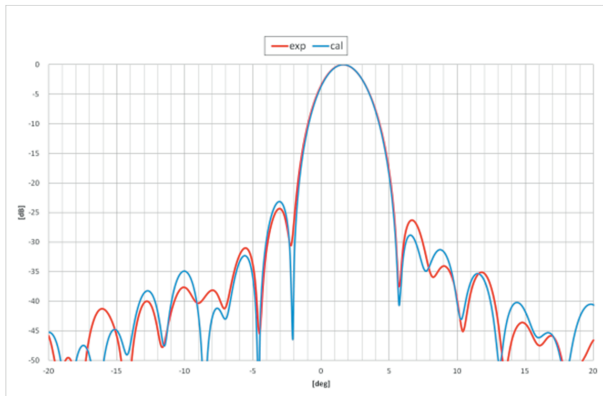
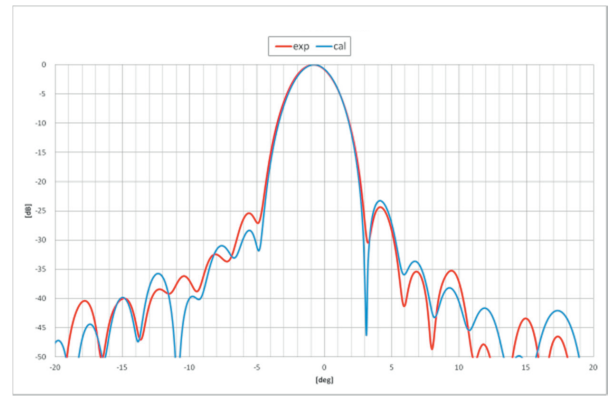


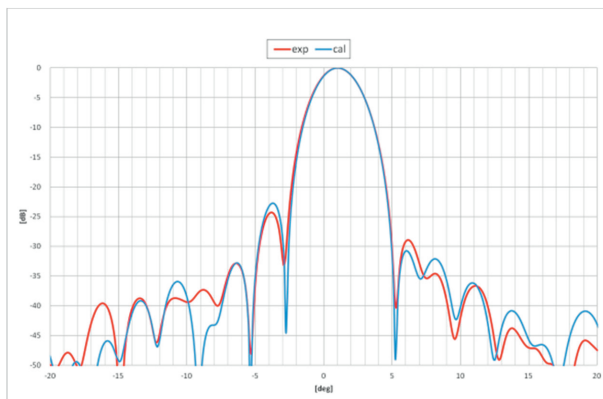
Fig. 18 Measurement results (beam position) cut angle is 30degree



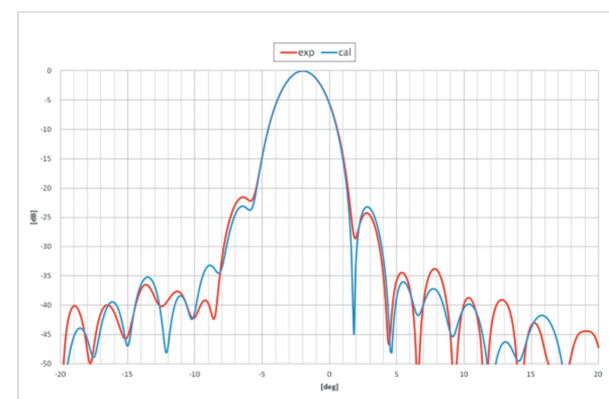
(a) Beam11



(c) Beam56



(b) Beam22



(d) Beam79

Fig. 19 Measurement results (radiation pattern) cut angle is 30 degree

4 Summary

We conducted experiments to confirm that the DBF/channelizer we developed is compatible with 100 elements and is capable of forming 100 beams. In conclusion, we found that the device is compatible with 100 elements and is capable of simultaneously forming 100 beams. In future studies, we are planning to realize the mounting of the DBF/channelizer on an antenna by making it smaller, power-saving and broadband-capable.

Acknowledgments

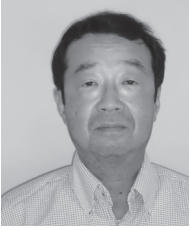
We thank the staff of the Research Institute for Sustainable Humanosphere, Kyoto University, including Dr. SHINOHARA and Dr. MITANI, for allowing us to use the advanced microwave energy transmission system.

This study was conducted to fulfill the research project commissioned by the Ministry of Internal Affairs and Communications titled “Research and development of Satellite Terrestrial Integrated Mobile Communication

System.” We thank those who supported this project.

References

- 1 M. Satoh, Y. Fujino, and T. Orikasa, “Characterization of Large-Scale Deployable Antenna Pattern Equipped with Engineering Test Satellite VIII on Orbit,” *Trans. IEICE on Communications (Japanese edition)*, Vol. J91-B, No.12, pp.1641–1643, Jan. 2008.
- 2 M. Satoh, T. Orikasa, and Y. Fujino, “Evaluation of Electrical performance for Large-Scale Deployable Reflector Antenna Equipped with Engineering Test Satellite VIII on Orbit,” *Trans. IEICE on Communication (Japanese edition)*, Vol. J94-B, No.3, pp.344–352, Jan. 2011.
- 3 T. Orikasa, M. Satoh, S. Yamamoto, and K. Kawasaki, “Error Correction Experiment of Radiation Pattern of Large Reflector Antenna,” *Special issue of NICT Journal*, Vol.61, No.1, 2014.
- 4 T. Orikasa, Y. Fujino, M. Satoh, and H. Tsuji, “Measurement experiment and evaluation of radiation patterns of the mesh reflector antenna mounted on communication satellite for hybrid mobile communication system,” *63rd International Astronautical Congress, IAC-12-B2.2.6*, Oct. 2012.
- 5 T. Orikasa, Y. Fujino, and H. Tsuji, “Experiment of satellite antenna with reflector and DBF/channelizer for STICS,” *IEICE Technical Report (Japanese edition)*, WPT-2012-45, May 2013.



Teruaki ORIKASA, Dr. Eng.

Senior Researcher, Space Communication
Systems Laboratory, Wireless Network
Research Institute
Space Communication, Antenna



Yoshiyuki FUJINO, Dr. Eng.

Professor, Department of Electrical and
Electronic Engineering, Faculty of Science
and Engineering, Toyo University/Former:
Senior Researcher, Space Communication
Systems Laboratory, Wireless Network
Research Institute (-April 2013)
Satellite Communication, Antenna, Wireless
Power Transmission